Cancer Management and Research

Dovepress

open access to scientific and medical research

Open Access Full Text Article

ORIGINAL RESEARCH

A Novel Pathological Scoring System for Hepatic Cirrhosis with Hepatocellular Carcinoma

This article was published in the following Dove Press journal:
Cancer Management and Research

Wei Dong[1,2,*]
Hua Yu[1,2,*]
Yu-Yao Zhu[1,2,*]
Zhi-Hong Xian[1,2]
Jia Chen[1,2]
Hao Wang[3]
Chun-Chao Shi[4]
Guang-Zhi Jin[5]
Hui Dong[1,2]
Wen-Ming Cong[1,2]

[1]Department of Pathology, Eastern Hepatobiliary Surgery Hospital, Second Military Medical University, Shanghai 200438, People's Republic of China; [2]Key Laboratory of Signaling Regulation and Targeting Therapy of Liver Cancer, Second Military Medical University, The Ministry of Education, Shanghai 200438, People's Republic of China; [3]Department of Hepatobiliary Diseases, Eastern Hepatobiliary Surgery Hospital, Second Military Medical University, Shanghai 200438, People's Republic of China; [4]Second Department of Hepatic Surgery, Eastern Hepatobiliary Hospital, Second Military Medical University, Shanghai 200438, People's Republic of China; [5]Department of Oncology, Tongren Hospital, Shanghai Jiao Tong University School of Medicine, Shanghai 200050, People's Republic of China

*These authors contributed equally to this work

Correspondence: Hui Dong
Department of Pathology, Eastern Hepatobiliary Surgery Hospital, Shanghai 200438, People's Republic of China
Email 13917078308@126.com

Wen-Ming Cong
Department of Pathology, Eastern Hepatobiliary Surgery Hospital, Shanghai 200438, People's Republic of China
Email wmcong@smmu.edu.cn

Purpose: This study aimed to propose an effective quantitative pathological scoring system and to establish nomogram to assess the stage of cirrhosis and predict postoperative survival of hepatocellular carcinoma (HCC) with cirrhosis patients after hepatectomy.

Methods: The scoring system was based on a retrospective study on 163 patients who underwent partial hepatectomy for HCC with cirrhosis. The clinicopathological and follow-up data of 163 HCC with cirrhosis patients who underwent hepatectomy in our hospital from 2010 to 2014 were retrospectively reviewed. A scoring system was established based on the total value of independent predictive factors of cirrhosis. The results were validated using 97 patients operated on from 2011 to 2015 at the same institution. Nomogram was then formulated using a multivariate Cox proportional hazards model to analyze.

Results: The scoring system was ultimately composed of 4 independent predictive factors and was divided into 3 levels. The new cirrhosis system score strongly correlated with Child–Pugh score (r=0.8058, P<0.0001) 3 months after surgery; higher cirrhosis system scores predicted poorer liver function and stronger liver damage 3 months after surgery. Then, a four-factor nomogram for survival prediction was established. The concordance indices were 0.79 for the survival-prediction nomogram. The calibration curves showed good agreement between predictions by the nomogram and actual survival outcomes.

Conclusion: This new scoring system of cirrhosis can help us predict the liver function and liver injury 3 months after surgery, and the nomogram enabled accurate predictions of risk of overall survival in patients of HCC with cirrhosis after hepatectomy.

Keywords: cirrhosis, hepatocellular carcinoma, HCC, pathology, scoring system, nomogram

Introduction

In more than 90% of cases, HCC develops within the background of established cirrhosis, and cirrhosis is the strongest predisposing factor for HCC.[1,2] Cirrhosis plays a vital role in determining and implementing an appropriate surgical strategy for HCC treatment; in addition, the severity of cirrhosis is closely associated with occurrence of liver-related events after surgery for HCC.[3] Cirrhosis decreases the functional reserve of the remaining liver, as well as the recovery of liver function.[4] Several portal-based staging systems have been used or proposed for grading of cirrhosis, including Histology Activity Index (HAI), Scheuer scoring system, histological semi-quantitative scoring system (SSS), Batts-Ludwig system, Metavir system, and Laennec system, etc.[5–12] Most of above staging systems have focused on grading hepatic fibrosis and inflammation, including only early cirrhosis, while in fact, a special histopathological sub-classification of cirrhosis is urgently needed in hepatic surgery based on the severity of cirrhosis.[5] The Laennec scoring system

submit your manuscript | www.dovepress.com
DovePress
http://doi.org/10.2147/CMAR.S223417

mainly according to the thickness of the predominant type of septa graded cirrhosis into 3 stages, which were purely morphology-based. Obviously, it is not easy to evaluate the percentage of liver parenchymal loss and the thickness of septa on small biopsy tissues. In the meantime, grading of resection specimens from cirrhotic patients with HCC has not been routinely used and verified. Qualitative or semi-quantitative assessments have a large subjective error; therefore, morphometry and image analysis applied to liver sections have been considered to be the gold standard because the intra assay variability is very low.[12] Those scoring systems are subject to the valid criticism that the stages represented by numbers do not accurately reflect equal units in terms of severity.[8] Therefore, based on morphometry and image analysis, we established a new quantitative scoring system, which is specifically applicable to patients of HCC with cirrhosis.

Inflammation and fibrosis can be used to assess the degree of cirrhosis. Portal inflammation is associated with liver injury and fibrogenic activity, and it is also strongly associated with regenerative activity at the portal-septal/lobular interface and with myofibroblast activity.[13] The extent of fibrosis is considered to be indicative of the stage of cirrhosis. MRP14 is a small calcium-binding protein with several immunological functions mainly involved in chronic inflammation[14] and has been proposed as one of the central inflammatory regulators capable of driving and responding to inflammation signals.[15] On one hand, MRP14 protein levels are significantly increased in response to cytokine stimulation, while on the other hand, it enhances inflammatory cascades by inducing leukocyte chemoattractants and the expression of pro-inflammatory cytokines.[15] MRP14 is also involved in fibrosis remodeling,[14] induced in response to liver injury, and acts as a powerful leukocyte chemoattractant.[16]

In this study, the pathological indexes and protein markers of inflammation and fibrosis were systematically screened, 6 parameters were finally selected for analysis. Average number of inflammatory cells in the portal area of the liver (NICP), proportion of hepatic fibrosis area (RFA), the density of the pseudolobules (DPL), MRP14 positive cell density(MRP14), the density of inflammatory cells in hepatic lobular area(DICH), average diameter of pseudolobules (ADP) were selected. These 6 parameters were quantitatively measured by the Image-Pro Plus v6.0 software. Diagnostic models were established by logistic regression analyses and externally validated in an independent testing group. In addition, we also evaluated the prognostic value of the new system and established the nomogram to predict overall survival in HCC patients with cirrhosis after liver resection.

Patients and Methods

Patients

We reviewed clinicopathological characteristics of 260 patients who underwent surgical resection and were diagnosed pathologically with HCC with cirrhosis at the Eastern Hepatobiliary Surgery Hospital from 2010 to 2015. Institutional review board approval and written informed consent from each patient were obtained. Hematoxylin-eosin (HE) stained slides, Masson-stained slides, and MRP14 immunohistochemically stained slides were prepared from formalin-fixed paraffin-embedded tissues of liver and reviewed by two experienced hepatopathologists (WM Cong and H Dong). Patients were randomly assigned to training group and testing group. We analyzed a training group consisting of 163 patients who underwent curative resection and classified them as Child–Pugh A (n=75), Child–Pugh B (n=40), or Child-Pugh C (n=48) according to Child–Pugh stage after 3 months of surgery. Additional 97 patients classified them as Child–Pugh A (n=47), Child–Pugh B (n=23), or Child–Pugh C (n=27) formed the testing group used to assess the validity of the model. Child–Pugh score 3 months after surgery was used as an indicator of liver function recovery. The morphology index and molecular markers of cirrhosis were chosen through systematic studies of histological characteristics of cirrhosis, cited references, and statistical analysis. We examined tissue area more than one centimeter away from the tumor, which would be more representative of the rest of the liver. The inclusion and exclusion criteria for patients and parameters in the current study were as follows: 1) preoperative liver function was Child–Pugh A and diagnosis of HCC with hepatitis B-induced cirrhosis; 2) there was no pre-surgical treatment for HCC including chemoembolization, radiofrequency ablation, or high-intensity focused ultrasound, which would confound the morphology of background liver; 3) cirrhosis was diagnosed according to the character of nodular regeneration surrounded by extensive septa, followed by parenchymal extinction and collapse of the liver structure;[17] 4) the selected parameters should be related to the liver function of postoperative patients. Each parameter was established from morphometric measurements.

Liver samples from various stages of cirrhosis were scored as an illustration in Figure S1.

Follow-Up

The patients were followed up once every 2–3 months during the first year after surgery and then every 3–6 months thereafter, tumor markers and liver function assessments were performed at each follow-up visit. The overall survival (OS) was defined as the length of time between surgery and death or the last follow-up examination.

H&E, Masson's Trichrome, Immunohistochemistry, and Parameter Score

The resected specimens were embedded in paraffin, and 4-μm-thick sections were cut and stained with hematoxylin and eosin (HE) and Masson's trichrome for routine light microscopy examination.[18,19] Immunohistochemical slices were stained with an automated immunostainer (Leica BOND-MAXTM, Darmstadt, Germany). The antibodies applied in our study were purchased from Changdao (Shanghai, China) or Maixin Biotech (Fuzhou, China) and were abbreviated and diluted, rabbit polyclonal antibody against calgranulin B (S100A9/MRP14) (sc-20173; Santa Cruz Biotechnology; 1/2500 dilution).[20] H&E staining was used to measure NICP and DICH; Masson staining was used to measure DPL, RFA, and ADP; and immunohistochemistry was used to measure the density of MRP14-positive cells.

The imaging system consisted of a Leica FC420 CCD camera connected to a Leica DM IRE2 microscope (Leica Microsystems Imaging Solutions, Cambridge, UK). Photographs of four fields were captured randomly from each slide under high-power magnification (100×) when measuring DICH and MRP14. All pseudolobules were captured under high-power magnification (100×) when measuring NICP. The entire area was captured from each slide under medium-power magnification (40×) when measuring RFA, and under low-power magnification (20×) when measuring DPL and ADP. All photographs were captured using Leica QW in Plus V3 software, the number and area for all photographs were counted and measured using Image-Pro Plus v6.0 software (Media Cybernetics, Bethesda, MD) for the three parameters of area sum, area, and sample. The number of inflammatory cells, MRP14 positive cells and fibrosis area were automatically measured by Iimage-Pro Plus's calibration measurement tool. The fibrotic region we selected was aniline blue staining region, the portal and inflammatory areas were extracted manually.

Statistical Analysis

Statistical analyses were carried out with IBM SPSS Statistics 22.0 software (IBM, Chicago, IL) and GraphPad Prism 5.01. Pearson's correlation and Spearman correlation test were used to analyze the relationship among the pathological parameters and different system score and stage. Differences between the measured values of each group were analyzed by Mann–Whitney test for each pathological parameter. In the training group, the measured values were used to perform receiver operating characteristic (ROC) analysis. The ROC curve showed sensitivity plotted against 1–specificity for each cut-off value and was used to determine the best cut-off of each parameter based on optimal sensitivity and specificity.[21] Multivariate associations with the diagnosis of cirrhosis were assessed by ordinal logistic regression models using generalized estimating equations with robust variance estimation and exchangeable correlation to account for correlations. The odds ratio (OR) was used as a coefficient of each parameter, the parameter grade minus one as the exponent of the coefficient, and the aggregate risk score was generated for each patient by summing the estimates of each factor.[22] Additionally, separate two-way analysis of covariance (ANCOVA) were performed using intraoperative blood loss, total clamp time, and resected liver diameter as covariates and pathological parameters of the system as dependent variables.[23] Survival curves were depicted using the Kaplan–Meier method and compared using the Log-rank test. Cox regression analysis was used for multivariate analyses.

A nomogram was formulated based on the results of multivariate analysis and by using the package of rms26 in R version 3.3.3 (http://www.r-project.org/). A final model selection was performed by a backward stepdown selection process with the Akaike information criterion. All statistical tests were two-sided and P values less than 0.05 were considered statistically significant.

Results

Results of Pathological Indicators Measurement

Six criteria compliant indicators were selected, and we analyzed the correlation between the pathological indicators and the Child–Pugh score. In the training group,

Child–Pugh score showed a statistically significant association with NICP (r=0.7247, P<0.001), RFA (r=0.7182, P<0.001), DPL (r=0.5617, P<0.001), MRP14 (r=0.6013, P<0.001), DICH (r=0.6484, P<0.001), and ADP (r=−0.3044, P<0.001). NICP, RFA, DPL, MRP14, and DICH were higher in high Child–Pugh stage than in low Child–Pugh stage, ADP was lower in high Child–Pugh stage than in low Child–Pugh stage (Figure S1).

Diagnostic Value and Histological Score

The histological score of training group is detailed in Table S1. Elements of system were classified on a scale of 3 grades as follows: NICP (A≤1102, 1102>B≤2519, C>2519); RFA (A ≤ 0.1192, 0.1192>B≤0.2040, C>0.2040); DPL (A≤ 13.13, 13.13>B≤23.67, C>23.67); density of MRP14 (A ≤113.4, 113.4>B≤185.5, C> 185.5), DICH (A ≤719.9, 719.9>B≤1500, C >1500.0); and ADP (A≥1764, 1764>B≥1213, C<1213).

The histological score is detailed in Table S1. Predictive effect was represented by area under the curve (AUC) of ROC curves. For Child–Pugh A/B the AUC was 0.8877 for NICP, 0.8820 for RFA, 0.9272 for DPL, 0.9272 for MRP14, 0.9500 for DICH, and 0.6107 for ADP. For Child–Pugh B/C the AUC was 0.8396 for NICP, 0.8135 for RFA, 0.8396 for DPL, 0.7451 for MRP14, 0.7266 for DICH, and 0.6209 for ADP (Figure S1). In addition, the best cut-off value was determined by the ROC curve. The sensitivity and specificity of each parameter for detection of liver function are summarized in Table S2. A high sensitivity (86.05%) coupled to low specificity (41.33%) for discriminating Child–Pugh A from Child–Pugh B was seen for ADP. A low sensitivity (60.42%) coupled to high specificity (97.50%) for discriminating Child–Pugh B from Child–Pugh C was seen for DICH. Both low sensitivity (52.08%) and low specificity (69.77%) for discriminating Child–Pugh B from Child–Pugh C were seen for ADP.

Construction of a Diagnostic Model

In univariable analysis, all of 6 indicators showed a statistically significant association with recovery of liver function, but ordinal logistic regression analysis showed that only NICP (P=0.011, OR=3.27), RFA (P=0.019, OR=3.07), DPL (P=0.032, OR=2.31), and MRP14 (P=0.001, OR=3.32) were associated with recovery of liver function (Table S3). NICP, RFA, DPL, and MRP14 were independent prognostic factors and were therefore used as the components of the cirrhosis scoring system. Multicollinearity analyses showed all of 4 parameters NICP (P=0.002), RFA (P<0.001), DPL (P=0.002), and MRP14 (P<0.001) in the model have statistical significance (Table S7). Covariance analyses showed no significant differences between the coefficients of independent prognostic factors for the cirrhosis model for different levels of intraoperative blood loss, total clamp time, and resected liver diameter (Table S4). The sensitivity and specificity of the cirrhosis score system were 100.00% and 82.67% (cut-off value of 6.85) for Child-A/Child-B group, 81.25% and 85.00% (cut-off value of 24.15) for Child-B/Child-C group (Table S2).

Model Evaluation in the Training Group

As shown in Figure S2, in the training group the Child–Pugh score correlated with new scoring system and other combinations of system factors, but the correlation coefficient of the system (r=0.8227, P<0.001) was higher than other combinations RFA+DPL+MRP14 (r=0.8167, P<0.001), NICP +DPL+MRP14 (r=0.8025, P<0.001), NICP+RFA+MRP14 (r=0.8096, P<0.001), NICP+RFA+DPL (r=0.8088, P<0.001); NICP+RFA (r=0.7922, P<0.001); NICP+DPL (r=0.7854, P<0.001), NICP+MRP14 (r=0.7705, P<0.001); RFA+DPL (r=0.7854, P<0.001), RFA+MRP14 (r=0.8001, P<0.001), DPL+MRP14 (r=0.7754, P<0.001). As shown in Figure S3, the AUC for Child–Pugh A/B and Child–Pugh B/C for cirrhosis scoring system (0.9500 and 0.8852) was higher than other combinations of system elements in the training group.

Table 1 The New Cirrhosis Scoring System

Variables	Grade		
	1	2	3
NICP	≤1102	1102<G1≤2519	>2519
RFA	≤0.1192	0.1192<G2≤0.2040	>0.2040
DPL (/cm^2)	≤13.13	13.13<G3≤23.67	>23.67
MRP14 (/mm^2)	≤113.4	113.4<G4≤185.5	>185.5
New Cirrhosis System Score=$OR_1^{G(NICP)-1}$+$OR_2^{G(RFA)-1}$+$OR_3^{G(DPL)-1}$ +$OR_4^{G(MRP14)-1}$			
(New Cirrhosis System Score=$3.27^{G(NICP)-1}$ +$3.07^{G(RFA)-1}$ +$2.31^{G(DPL)-1}$ +$3.32^{G(MRP14)-1}$)			
System Grade: I≤6.85, 6.85<II≤24.15, IV>24.15			

Notes: OR_1, OR value of NICP; OR_2, OR value of RFA; OR_3, OR value of DPL; OR_4, OR value of MRP14; G(NICP), grade of NICP; G(RFA), grade of RFA; G(DPL), grade of DPL; G(MRP14), grade of MRP14.

Cirrhosis Stage Scoring System

The standard cirrhotic scoring system was defined according to the following equation (Table 1):

Cirrhosis Score=$3.27^{G(NICP)-1}$+$3.07^{G(RFA)-1}$+$2.31^{G-(DPL)-1}$+$3.32^{G(MRP1)-14}$

Cirrhosis Stage was classified as follows: I≤6.85, 6.85>II≤24.15, III>24.15. The pathological features of each cirrhotic are shown in Figure 1.

Parameters and Model Evaluation in the Testing Group

For the testing group, the clinicopathological features were summarized in Table S5 and the different systems' scores were summarized in Table S6. As shown in Figure S6, the component factors of cirrhosis scoring system have good correlation with the serum indexes.

The correlation between the new cirrhosis system score and TIBL (P<0.001), ALT (P=0.008), AST (P<0.001), ALP (P<0.001), ALB (P=0.003), PT (P<0.001), Cre (P<0.001), ascitic score (P<0.001), and encephalopathy score (P<0.001) showed statistical significance. The Laennec score system was only correlated with PT (P=0.019) (Figure S4, Table S8).

There was a very close relationship between the stage of cirrhosis system and Child–Pugh stage (r= 0.8048, P<0.001), as well as correlation between the cirrhosis system score and Child–Pugh score (r=0.8058, P<0.001) and MELD score (r =0.666, P<0.001) 3 months after surgery, with higher

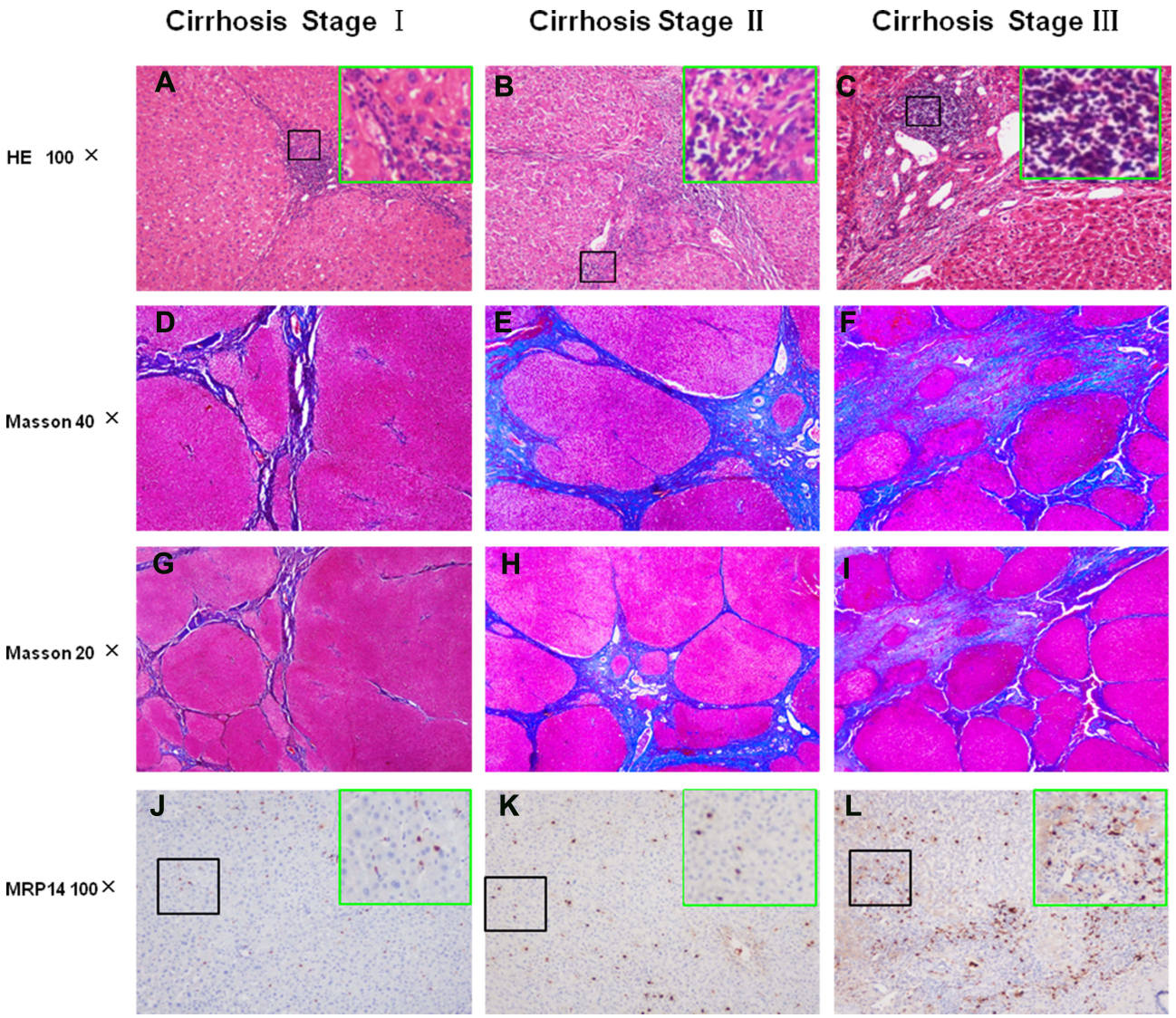

Figure 1 Four histological items for evaluation of cirrhosis system. H&E stain shows NICP of Cirrhosis Stage 1 (**A**), Cirrhosis Stage 2 (**B**), Cirrhosis Stage 3 (**C**) (**F**); Masson stain shows RFA of Cirrhosis Stage 1 (**D**), Cirrhosis Stage 2 (**E**), Cirrhosis Stage 3 (**F**), DPL of Cirrhosis Stage 1 (**G**), Cirrhosis Stage 2 (**H**), Cirrhosis Stage 3 (**I**); MRP14 stain shows of Cirrhosis Stage 1 (**J**), Cirrhosis Stage 2 (**K**), Cirrhosis Stage 3 (**L**). Black boxes, representative views of tissue; green boxes, enlarged representative views.

correlation coefficient than any of the four independent variables. There was a low correlation between the Laennec score and Child–Pugh scores (r=0.2779, P=0.0059), MELD scores (r=0.3271, P=0.0011) and between the Laennec stage and Child–Pugh stage (r=0.1872, P=0.0663) (Figure S5, Figure S6). The AUC for cirrhosis I/II and cirrhosis II/IV for Child–Pugh scores were 0.840 (P<0.001) and 0.913 (P<0.001) in the testing group, suggesting that the model has good evaluation efficiency, and the efficiency was higher for cirrhosis II/III than cirrhosis I/II (Figure S7).

Prognostic Significance

At the time of last follow-up, among 260 patients in the training and testing group, 112 had died, the median OS was 40.5 months (range, 3.4 to 82.4 months) and overall survival of patients stratified by the Cirrhosis stage system was summarized in the Table S9. Kaplan–Meier curves demonstrated that the new cirrhosis system and Laennec system were significantly associated with OS in both training and testing group (Figure 2). The Laennec scoring system was statistically significant at univariate analysis, but it was not statistically significant at multivariate analysis. The results of the univariate and multivariate analysis are listed in Table 2. Multivariate analyses demonstrated that serum AFP, MVI, TNM, and new cirrhosis scores were independent risk factors for HCC with cirrhosis OS (Table 2).

Prognostic Nomogram for OS

The prognostic nomogram that integrated all significant independent factors for OS in the combination of training

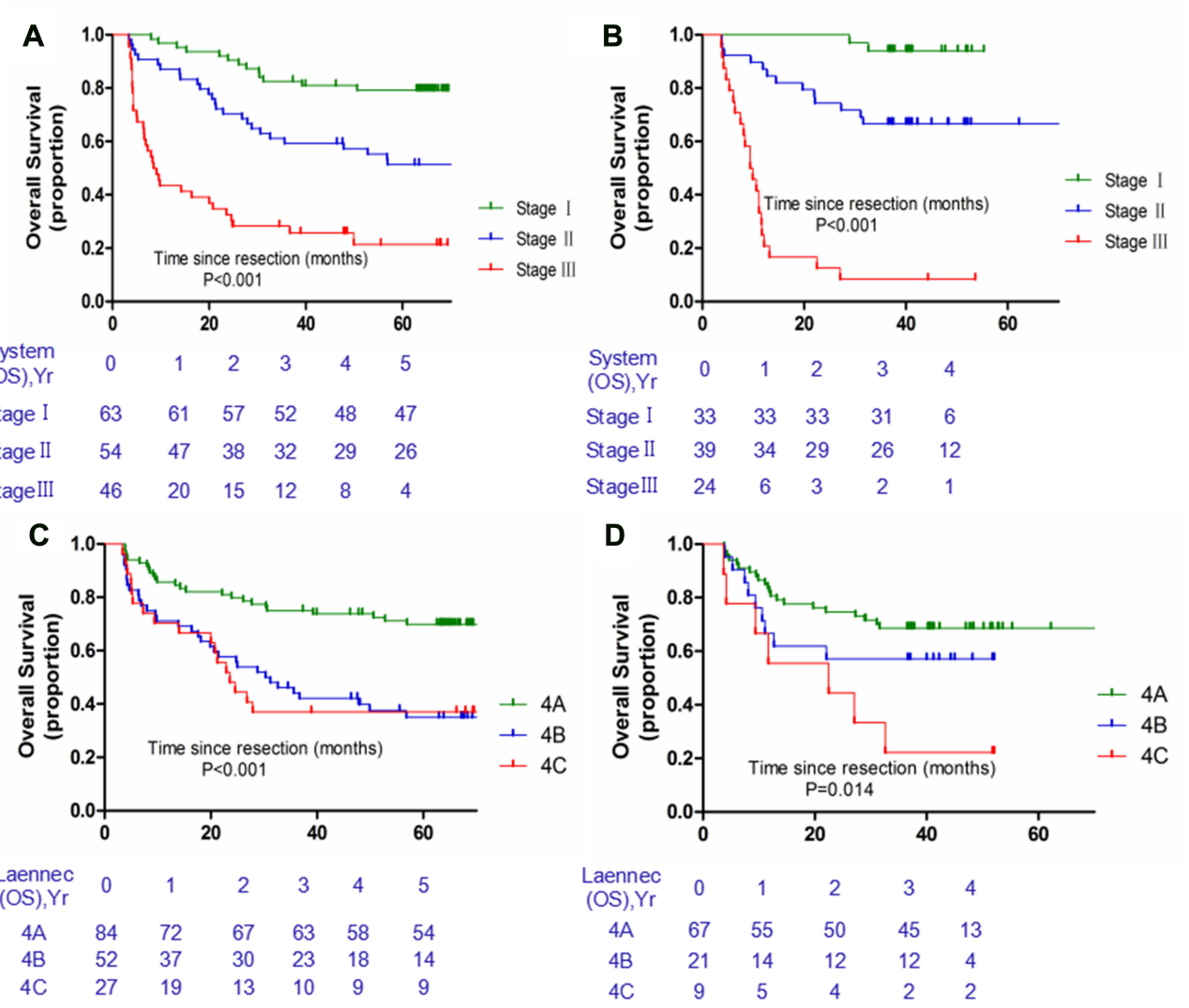

Figure 2 Kaplan–Meier survival curves of OS differences among patients in combination of training and testing group. Cirrhosis stage of training group (**A**) and testing group (**B**), Laennec stage of training group (**C**), and testing group (**D**).

and testing group is shown in Figure 3. The C-index for OS prediction was 0.79 (95% CI, 0.73 to 0.85). The calibration plot for the probability of survival at 1, 3, or 5 years after surgery showed an optimal agreement between the prediction by nomogram and actual observation (Figure 4).

Discussion

Diagnosing the severity of disease is an essential component of the baseline assessment of any disease. At the same time, cirrhosis plays a vital role in determining and implementing an appropriate surgical strategy for HCC treatment, and the severity of cirrhosis is closely associated with the occurrence of liver-related events after surgery for HCC.[3] Although several staging systems for cirrhosis have been proposed, conventional systems combine all severity levels into a single category. However, there are variations in both the histopathology of cirrhosis and the severity of disease. Only the Laennec system subdivides cirrhosis to recognize the variability in severity.[5] However, the Laennec system in our study was of limited value in the assessment of cirrhosis in HCC patients. Accordingly, the aim of this study was to propose an effective quantitative pathological scoring system to predict the post-operative liver function and to establish nomogram to predict postoperative survival of HCC with cirrhosis patients after hepatectomy.

Definition of the grades of severity of each lesion should be as precise as possible. In general, more complex systems have the capability to provide more information than simple ones.[8] The new cirrhosis model consists of four quantitative parameters—NICP, RFA, DPL, and MRP14. All of the parameters are measured through the software. In order to get a more accurate assessment, the system was established based on the OR and the grade of each parameter (ie, cirrhosis system score=$OR_1^{G(NICP)-1}$+$OR_2^{G(RFA)-1}$+$OR_3^{G(DPL)-1}$ +$OR_4^{G(MRP14)-1}$). The coefficients of the model in the scale are derived statistically so that appropriate weights are given to variables according to their relative risk value. Due to the large subjective error of qualitative or semi-quantitative evaluation, morphological and image analysis of liver slices is considered as the gold standard because of its low intrinsic variability.[12] Meanwhile, the establishment of quantitative grading system can promote the new software-assisted system in the pathological application to improve work efficiency and accuracy.

Table 2 Univariate and Multivariate Analyses of Factors Associated with OS in Combined Training and Testing Cohorts

Factors	Univariate			Multivariate		
	HR	95% CI	P-value	HR	95% CI	P-value
Age: years	1.025	1.005–1.046	**0.012**			
Sex: male vs female	0.910	0.536–1.545	0.727			
Tumor Size: cm	1.111	1.066–1.157	**<0.001**			
Tumor Number: Single vs Multiple	0.599	0.406–0.884	**0.01**			
Serum AFP, μg/L	1.001	1.000–1.001	**<0.001**	1.000	1.000–1.001	**0.031**
Serum CEA, μg/L	1.062	1.027–1.098	**<0.001**			
Serum CA 19–9, U/mL	1.005	1.000–1.011	0.066			
Serum TBIL, μmol/L	1.007	0.997–1.016	0.188			
Serum ALB, g/L	0.962	0.923–1.004	0.076			
Serum ALT, U/L	1.000	0.997–1.002	0.776			
Serum AST, U/L	1.000	0.997–1.002	0.928			
Serum GGT, U/L	1.003	1.002–1.004	**<0.001**			
Serum ALP, U/L	1.008	1.004–1.011	**<0.001**			
Serum PLT, $\times10^9$/L	0.996	0.993–1.000	**0.028**			
Serum PT, S	1.217	1.061–1.395	**0.005**			
Serum Cre, μmol/L	1.005	0.998–1.012	0.192			
Micro-vascular invasion: no vs yes	0.662	0.454–0.965	**0.032**	1.613	1.006–2.585	**0.047**
Laennec Score	1.763	1.401–2.218	**<0.001**			
TNM: I vs II vs III vs IV	1.656	1.360–2.016	**<0.001**	1.540	1.201–1.975	**0.001**
New Cirrhosis Score	1.079	1.062–1.095	**<0.001**	1.072	1.054–1.090	**<0.001**

Notes: TNM, cancer tumor-node-metastasis classification system; statistically significant values are bold.

Abbreviations: OS, overall survival; CI, confidence interval; AFP, preoperative level of serum α-fetoprotein; CEA, preoperative level of serum carcinoembryonic antigen; CA19-9, preoperative level of serum cancer antigen 19-9.

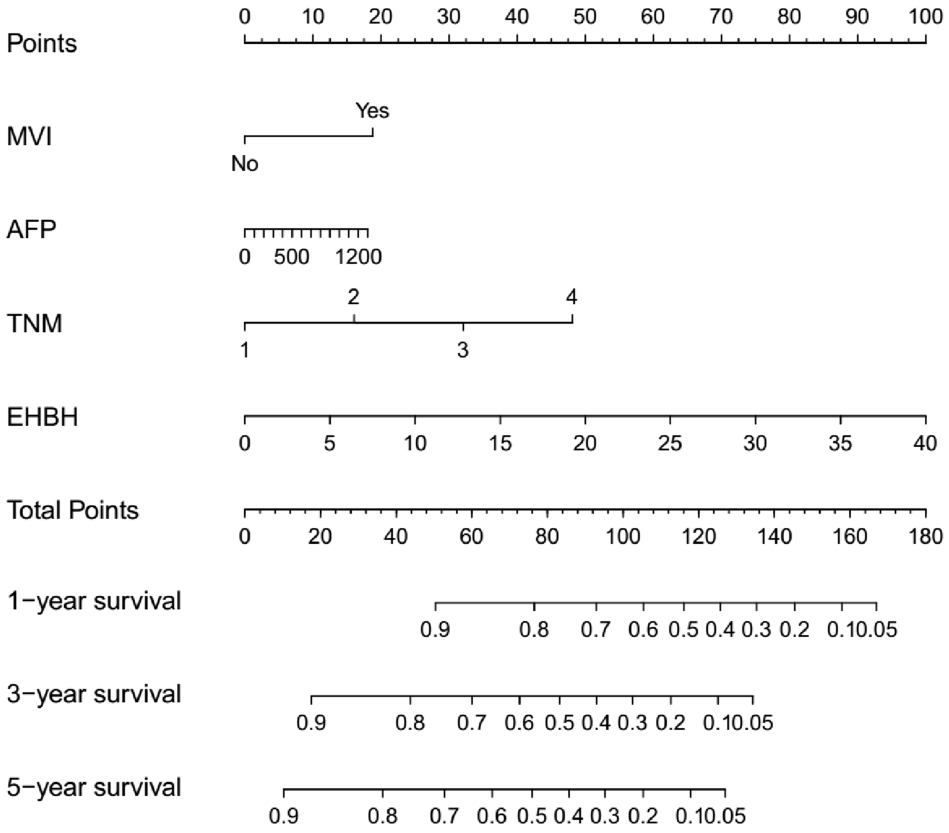

Figure 3 HCC with cirrhosis survival nomogram. (To use the nomogram, an individual patient's value is located on each variable axis, and a line is drawn upward to determine the number of points received for each variable value. The sum of these numbers is located on the Total Points axis, and a line is drawn downward to the survival axes to determine the likelihood of 1-, 3-, or 5-year survival). MVI, microvascular invasion.

Liver function generally returns to a more stable level within 12 weeks after partial hepatectomy.[24] The main influencing factor of liver function after 3 months is pathological basis lesion, the liver function index after 3 months of surgery can better reflect the actual state of the liver. So we chose the liver function 3 months after surgery as the evaluation criteria. Therefore, this system can predict the actual state of the liver and the evolution of liver function. This pathology system provides new reference indicators for clinical evaluation of cirrhosis soon after surgery, this problem has not been solved in traditional systems. Ideally, there should also be a demonstrable correlation with clinical outcome.[8] Thus, we built the model according to the postoperative liver function recovery to screen index.

In the present study, we found that MRP14 was associated with the liver function (with Child–Pugh, r=0.7206, P<0.0001), serum index (TBIL, ALT, AST, ALP, PT), and clinical parameters (ascites, encephalopathy) 3 months after surgery in cirrhosis with HCC. Inflammation is not only a factor of severity of disease but also reflects ongoing disease activity and is one of the most potentially responsive parameters to therapy. Therefore, including inflammatory assessment in the system and the system has the function of monitoring the treatment response. We found that NICP correlated with the recovery of liver function (with Child–Pugh, r=0.7143, P<0.0001), serum index (TBIL, ALT, AST, ALP, A/G, PT, Cre), and clinical parameters (ascites, encephalopathy) after surgery in cirrhosis with HCC. The extent of fibrosis was considered to be indicative of the stage of fibrosis and cirrhosis. In our study, RFA correlated with the recovery of liver function (with Child–Pugh, r=0.6627, P<0.0001), serum index (TBIL, ALT, AST, ALP, Cre), and DPL correlated with the recovery of liver function (with Child–Pugh, r=0.6167, P<0.0001), serum index (TBIL, ALT, AST, ALP, ALB, PT, Cre), and clinical parameters (ascites, encephalopathy) after surgery in cirrhosis with HCC (Table S8). These four parameters not only reflect the morphological changes but also reflect the liver damage and liver function. The

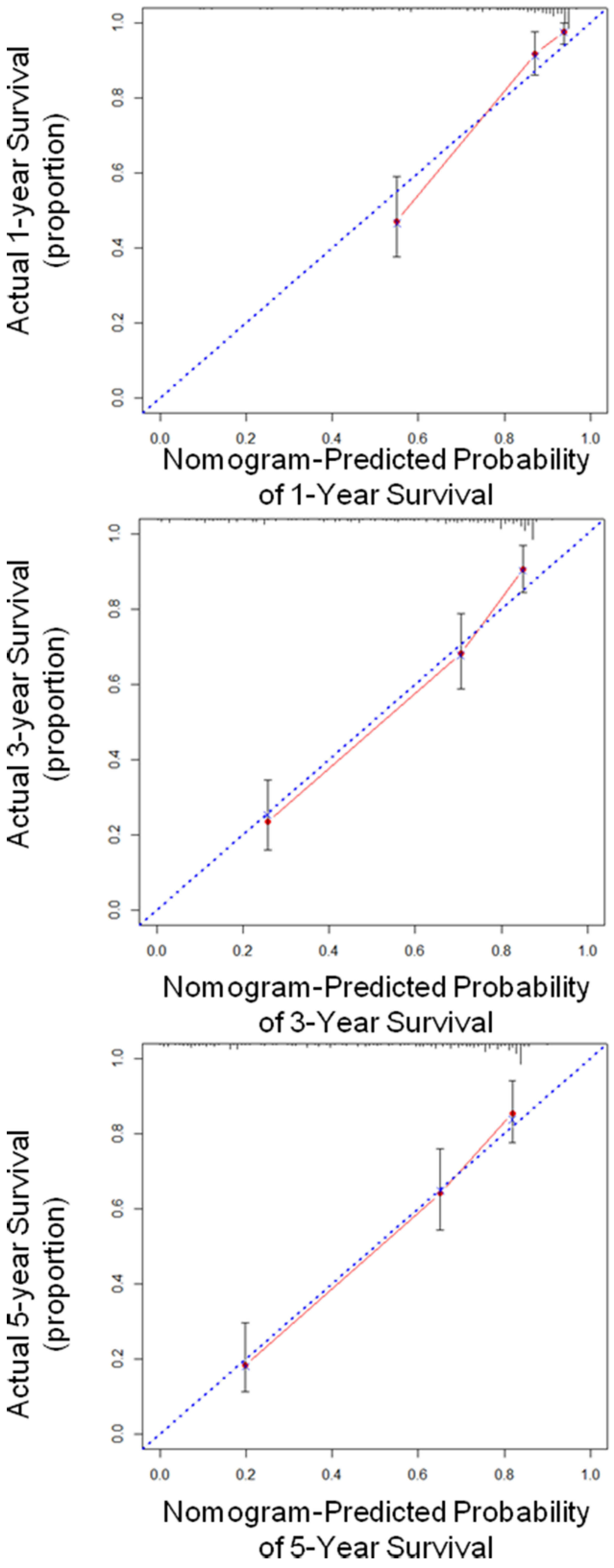

Figure 4 The calibration curve for predicting patient survival at (**A**) 1 year, (**B**) 3 years, and (**C**) 5 years in combined training and testing cohort. Nomogram-predicted probability of overall survival is plotted on the x-axis; actual overall survival is plotted on the y-axis.

correlation and diagnostic efficiency of the cirrhosis system were higher than combinations of part of elements and any individual element at the same time (Figure S3). The new cirrhosis system score value strongly correlated with Child–Pugh score value (r=0.8227, P<0.001) in training group, and in testing group the system score value strongly correlated the Child–Pugh score value (r=0.8058, P<0.0001), and serum index value of TBIL (r=0.6370, P<0.001), PT (r=0.6405, P<0.001) and a statistically significant correlation with value of ALT (r=0.2678, p=0.008), AST (r=0.4861, P<0.0001), ALP (r=0.3922, P=0.0002), ALB (r=−0.3012, P=0.0027), Cre (r=0.3903, P<0.0001), Ascitic (r=0.3772, P=0.0001), Encephalopathy (r=0.4537, P<0.0001) 3 month after surgery (Table S8), suggested that the new cirrhosis can reflect the liver recovery of liver function and may reflect the liver injury and blood coagulation and liver function compensation at 3 months after operation for HCC with cirrhosis. Higher cirrhosis system scores predicted poorer liver function and stronger liver damage 3 months after surgery.

The degree of liver damage is another important prognostic factor after HCC surgery.[25] Risk factors for morbidity after liver resection include blood loss volume, resected liver volume, and total clamp time.[26–28] ANCOVA is defined more purely as a continuous variable used to control for its effect when testing categorical independent variables.[29] Therefore, we used intraoperative blood loss, total clamp time, and resected liver diameter as covariates when performing covariance to detect statistical significance between the coefficients of independent prognostic factors for the new cirrhosis model when excluding covariates. Covariance analysis showed that liver damage had no efficacy among the four pathological parameters of the cirrhosis scoring model.

The relative diagnostic importance of each factor depends on the features of the patients in the training sample, as do the independent variables remaining after stepwise selection.[30] The Laennec scoring system grew from the recognition that systems in use for histologic evaluation of liver fibrosis and cirrhosis may not be appropriately used for the unique lesions of cirrhosis in HCC patients. The possible reason why the Laennec system has a poor correlation with liver function recovery was ignoring the effects of inflammation and the special environment of cirrhosis in HCC patients. Similarly, the applicability of the new cirrhosis scoring system is limited by the fact that it was established and validated on the basis of cirrhosis patients with HCC treated by surgical

resection. However, it is increasingly recognized that the importance of grading cirrhosis in patients with HCC is due to its impact on prognosis.

In the present study, Kaplan–Meier analyses revealed that high cirrhosis stage was significantly linked to poor OS after surgical resection in HCC patients in both the training and testing groups. Meanwhile, the new cirrhosis system was a significant independent prognostic factor for OS. In our prognostic nomogram, the cirrhosis system was shown to be a poor prognostic factor that shortened OS. The nomogram also include important features of the tumor, including the serum AFP, MVI, and TNM. The C-indices of this nomogram was 0.79, and this nomogram also performed well in predicting long-term survival.

There are several limitations to this study. First, the nomogram was established based on data obtained from a single institution in China. Second, whether this cirrhosis scoring system and nomogram can be applied to liver biopsy remains to be determined.

In conclusion, we established a quantitative scoring system for cirrhosis in patients with HCC by measuring morphological and molecular markers associated with postoperative liver function. The prognostic nomogram was then developed to predict overall survival after hepatectomy. Taken together, these tools can provide a valuable reference for clinical assessment of the risks of postoperative liver function recovery and long-term survival.

Abbreviations

ADP, average diameter of pseudolobules; AFP, α-fetoprotein; ALB, albumin; ALP, alkaline phosphatase, ALT, alanine aminotransferase; ANCOVA, separate two-way analyses of covariance; AST, aspartate transaminase; AUC, area under the curve; A/G, albumin/globulin; CA19-9, cancer antigen 19-9; CEA, carcinoembryonic antigen; Cre, creatinine; DICH, density of inflammatory cells per square millimeter in hepatic area; DPL, density of pseudolobules per square centimeter; HCC, hepatocellular carcinoma; HE, hematoxylin-eosin; MELD, the model for end-stage liver disease; NICP, number of inflammatory cells in the portal area; OR, odds ratio; PT, prothrombin time; RAGE, advanced glycation end products; RFA, ratio of hepatic fibrosis area divided by total area; ROC, receiver operating characteristic; TNM, tumor-node-metastasis classification system; TBIL, total bilirubin.

Contributor Information

Wei Dong, Email: well_dw@126.com; Hua Yu, Email: gwsandyh@sohu.com; Yuyao Zhu, Email: zhuyuyao111@163.com; Jia Chen, Email: cherrycd@163.com; Zhihong Xian, Email: xianzh7210@163.com; Chunchao Shi, Email: shiccdg@163.com; Guangzhi Jin, Phone: 86-20-61,642,147, Email: jgzhi@-hotmail.com; Hui Dong, Email: 13,917,078,308@126.com; Wenming Cong, Phone: 86-20-61,642,147, Email: wmcong@smmu.edu.cn.

Data Sharing Statement

All data generated or analyzed during this study are included in this article and its Additional files.

Ethics Approval and Consent Statement

The research protocol was approved by the Ethics Committee Shanghai Eastern Hepatobiliary Surgery Hospital. All the patients provide written informed consent.

Consent for Publication

All authors have seen the manuscript and approved to submit to your journal.

Acknowledgments

The authors gratefully acknowledge Professor Swan N. Thung, Department of Pathology, Mount Sinai Health System, NY, USA, for suggestions and comments on the manuscript.

Author Contributions

Study concept design: Wen-Ming Cong, Guang-Zhi Jin and Hui Dong; HE stain and Masson's trichrome stain: Wei Dong, Hua Yu, Yu-Yao Zhu; Immunohistochemistry stain: Wei Dong, Guang-Zhi Jin, Zhi-Hong Xian; Acquisition of data, interpretation of data: Wei Dong, Hua Yu, Yu-Yao Zhu, Guang-Zhi Jin, Jia Chen, Hao Wang, Chun-Chao Shi; All authors contributed to data analysis, drafting and revising the article, gave final approval of the version to be published, and agree to be accountable for all aspects of the work.

Funding

This study was supported by grants from the National Natural Science Foundation of China [grant numbers: 81472278, 81272662, 81472769]; and Funds for Creative Research Groups of National Natural Science Foundation of China [grant number: 81521091].

Disclosure

The authors declare that they have no competing interests.

References

1. Bruix J, Gores GJ, Mazzaferro V. Hepatocellular carcinoma: clinical frontiers and perspectives. *Gut*. 2014;63(5):844–855. doi:10.1136/gutjnl-2013-306627
2. Josep M, Llovet AB, Jordi B. Hepatocellular carcinoma. *Lancet*. 2003;362(9399):1907–1917. doi:10.1016/S0140-6736(03)14964-1
3. Zhang EL, Zhang ZY, Wang SP, et al. Predicting the severity of liver cirrhosis through clinical parameters. *J Surg Res*. 2016;204(2):274–281. doi:10.1016/j.jss.2016.04.036
4. Wagener G. Assessment of hepatic function, operative candidacy, and medical management after liver resection in the patient with underlying liver disease. *Semin Liver Dis*. 2013;33(03):204–212. doi:10.1055/s-0033-1351777
5. Kim MY, Cho MY, Baik SK, et al. Histological subclassification of cirrhosis using the Laennec fibrosis scoring system correlates with clinical stage and grade of portal hypertension. *J Hepatol*. 2011;55(5):1004–1009. doi:10.1016/j.jhep.2011.02.012
6. Bedossa P, Poynard T. An algorithm for the grading of activity in chronic hepatitis C. The METAVIR cooperative study group. *Hepatology*. 1996;24:289–293.
7. Ishak K, Baptista A, Bianchi L, et al. Histological grading and staging of chronic hepatitis. *J Hepatol*. 1995;22:696–699. doi:10.1016/0168-8278(95)80226-6
8. Goodman ZD. Grading and staging systems for inflammation and fibrosis in chronic liver diseases. *J Hepatol*. 2007;47:598–607. doi:10.1016/j.jhep.2007.07.006
9. Batts KP, Ludwig J. Chronic hepatitis an update on terminology and reporting. *Am J Surg Pathol*. 1995;19(12):1409–1417. doi:10.1097/00000478-199512000-00007
10. Albillos A, de la Hera A, Gonzalez M, et al. Increased lipopolysaccharide binding protein in cirrhotic patients with marked immune and hemodynamic derangement. *Hepatology*. 2003;37(1):208–217. doi:10.1053/jhep.2003.50038
11. Knodell RG, Ishak KG, Black WC, et al. Formulation and application of a numerical scoring system for assessing histological activity in asymptomatic chronic active hepatitis. *Hepatology*. 1981;1(5):431–435. doi:10.1002/hep.1840010511
12. Chevallier M, Guerret S, Chossegros P, Gerard F, Grimaud JA. A histological semiquantitative scoring system for evaluation of hepatic fibrosis in needle liver biopsy specimens: comparison with morphometric studies. *Hepatology*. 1994;20(2):349–355. doi:10.1002/hep.1840200213
13. Carotti S, Vespasiani-Gentilucci U, Perrone G, Picardi A, Morini S. Portal inflammation during NAFLD is frequent and associated with the early phases of putative hepatic progenitor cell activation. *J Clin Pathol*. 2015;68(11):883–890. doi:10.1136/jclinpath-2014-202717
14. Bargagli E, Olivieri C, Cintorino M, et al. Calgranulin B (S100A9/MRP14): a key molecule in idiopathic pulmonary fibrosis? *Inflammation*. 2011;34(2):85–91. doi:10.1007/s10753-010-9210-7
15. Swindell WR, Johnston A, Xing X, et al. Robust shifts in S100a9 expression with aging: a novel mechanism for chronic inflammation. *Sci Rep*. 2013;3(1):1215. doi:10.1038/srep01215
16. Moles A, Murphy L, Wilson CL, et al. A TLR2/S100A9/CXCL-2 signaling network is necessary for neutrophil recruitment in acute and chronic liver injury in the mouse. *J Hepatol*. 2014;60(4):782–791. doi:10.1016/j.jhep.2013.12.005
17. Ferrell L. Liver pathology: cirrhosis, hepatitis, and primary liver tumors. *Update Diagn Prob Mod Pathol*. 2000;13:679–704.
18. Ran RJ, Zheng XY, Du LP, Zhang XD, Chen XL, Zhu SY. Upregulated inflammatory associated factors and blood-retinal barrier changes in the retina of type 2 diabetes mellitus model. *Int J Ophthalmol*. 2016;9(11):1591–1597. doi:10.18240/ijo.2016.11.09
19. Mao H, Su P, Qiu W, Huang L, Yu H, Wang Y. The use of Masson's trichrome staining, second harmonic imaging and two-photon excited fluorescence of collagen in distinguishing intestinal tuberculosis from Crohn's disease. *Colorectal Dis*. 2016;18:1172–1178. doi:10.1111/codi.13400
20. Jin GZ, Dong W, Dong H, et al. The diagnostic and prognostic value of MRP8/MRP14 in intrahepatic cholangiocarcinoma. *Oncotarget*. 2015;6:39357–39364. doi:10.18632/oncotarget.5329
21. Kaur S, Smith LM, Patel A, et al. A Combination of MUC5AC and CA19-9 improves the diagnosis of pancreatic cancer: a multicenter study. *Am J Gastroenterol*. 2016.
22. Hristova R, Pompili C, Begum S, et al. An aggregate score to predict the risk of large pleural effusion after pulmonary lobectomy. *Eur J Cardio Thor Surg*. 2015;48(1):72–76. doi:10.1093/ejcts/ezu413
23. Andrade EH, Rizzo LB, Noto C, et al. Hair cortisol in drug-naive first-episode individuals with psychosis. *Revista Brasileira De Psiquiatria*. 2016;38(1):11–16. doi:10.1590/1516-4446-2014-1634
24. Lock JF, Malinowski M, Seehofer D, et al. Function and volume recovery after partial hepatectomy: influence of preoperative liver function, residual liver volume, and obesity. *Langenbecks Arch Surg*. 2012;397(8):1297–1304. doi:10.1007/s00423-012-0972-2
25. Ishizawa T, Hasegawa K, Aoki T, et al. Neither multiple tumors nor portal hypertension are surgical contraindications for hepatocellular carcinoma. *Gastroenterology*. 2008;134(7):1908–1916. doi:10.1053/j.gastro.2008.02.091
26. Smyrniotis VE, Kostopanagiotou GG, Contis JC, et al. Selective hepatic vascular exclusion versus Pringle maneuver in major liver resections: prospective study. *World J Surg*. 2003;27(7):765–769. doi:10.1007/s00268-003-6978-8
27. Ishizuka M, Kubota K, Kita J, Shimoda M, Kato M, Sawada T. Duration of hepatic vascular inflow clamping and survival after liver resection for hepatocellular carcinoma. *Br J Surg*. 2011;98(9):1284–1290. doi:10.1002/bjs.7567
28. Aramaki O, Takayama T, Higaki T, et al. Decreased blood loss reduces postoperative complications in resection for hepatocellular carcinoma. *J Hepatobiliary Pancreat Sci*. 2014;21(8):585–591. doi:10.1002/jhbp.101
29. Hutmacher MM, Kowalski KG. Covariate selection in pharmacometric analyses: a review of methods. *Br J Clin Pharmacol*. 2015;79(1):132–147. doi:10.1111/bcp.12451
30. Tateishi R, Yoshida H, Shiina S, et al. Proposal of a new prognostic model for hepatocellular carcinoma: an analysis of 403 patients. *Gut*. 2005;54:419–425. doi:10.1136/gut.2003.035055